Turczaninowia 28, 4: 195–213 (2025)
https://www.doi.org/10.14258/turczaninowia.28.4.22
http://turczaninowia.asu.ru

ISSN 1560–7259 (print edition)
TURCZANINOWIA
ISSN 1560–7267 (online edition)

УДК 582.579.2:581.961+577.21

Iris cryptoruthenica sp. nov. (Iridaceae): a cryptic lineage within the morphotype *Iris ruthenica* revealed by chloroplast and rDNA barcoding and karyosystematic evidence

P. M. Zhurbenko[1, 7*], C. A. Wilson[6, 16], V. I. Dorofeyev[1, 8], T. V. Matveeva[4, 5, 15], V. V. Kotseruba[1, 9], V. S. Shneyer[1, 10], E. D. Badaeva[2, 12], M. V. Skaptsov[3, 13], A. I. Shmakov[3, 14], A. V. Rodionov[1, 4, 11], N. B. Alexeeva[1, 17]

[1] *Komarov Botanical Institute RAS, Prof. Popova St., 2, St. Petersburg, 197022, Russian Federation*

[2] *Vavilov Institute of General Genetics, Russian Academy of Sciences, Gubkina St., 3, Moscow, 119991, Russian Federation*

[3] *Altai State University, Lenina Pr., 61, Barnaul, 656049, Russian Federation*

[4] *St. Petersburg State University, University Emb., 7, 9, St. Petersburg, 199034, Russian Federation*

[5] *All-Russian Institute of Plant Protection, Podbelskogo Pr., 3, St. Petersburg – Pushkin, 196608, Russian Federation*

[6] *University of California, Berkeley, 1001 Valley Life Sciences No. 2465, Berkeley, California, CA 94720-2465, USA*

[7] *E-mail: pj_28@mail.ru; ORCID iD: https://orcid.org/0000-0002-2102-4568*

[8] *E-mail: vdorofeyev@yandex.ru; ORCID iD: https://orcid.org/0000-0002-3642-197X*

[9] *E-mail: viola.kotseruba@gmail.com; ORCID iD: https://orcid.org/0000-0003-1872-2223*

[10] *E-mail: shneyer@rambler.ru; ORCID iD: https://orcid.org/0000-0002-6122-6770*

[11] *E-mail: avrodionov@mail.ru; ORCID iD: https://orcid.org/0000-0003-1146-1622*

[12] *E-mail: katerinabadaeva@gmail.com; ORCID iD: https://orcid.org/0000-0001-7101-9639*

[13] *E-mail: mr.skaptsov@mail.ru; ORCID iD: https://orcid.org/0000-0002-4884-0768*

[14] *E-mail: alex_shmakov@mail.ru; ORCID iD: https://orcid.org/0000-0002-1052-4575*

[15] *E-mail: radishlet@gmail.com; ORCID iD: https://orcid.org/0000-0001-8569-6665*

[16] *E-mail: cawilson@berkeley.edu; ORCID iD: https://orcid.org/0000-0003-0622-7479*

[17] *E-mail: a_nina@bk.ru; ORCID iD: https://orcid.org/0000-0002-4670-3110*

** Corresponding author*

Keywords: angiosperms, barcoding, cryptic species, chromosome counts, flow cytometry, iris, morphological crypsis, plants.

Summary. *Iris ruthenica* is a widespread Siberian species occurring in both boreal forest and steppe habitats, yet its genetic structure has remained poorly understood. During a survey of *I. ruthenica* in the Altai Mountain Country, we detected a cryptic lineage that is morphologically indistinguishable from *I. ruthenica* s. str. but differs in chromosome number. All Russian populations examined to date have $2n = 84$, whereas the cryptic lineage has $2n = 42$, and flow cytometry shows a corresponding difference in genome size (1C = 4.025 ± 0.110 pg vs. 1C = 2.135 ± 0.020 pg). Comparative analyses of chloroplast markers spanning the *atpB–accD* and *rpl2–matK* intervals (including *atpB*, *accD*, *psbA*, *rbcL*, *rpl2*, *rps19*, *matK*, and *ycf1*) revealed a p-distance of ~ 0.5 % between the two lineages, a level of divergence that falls within the range observed between recognized *Iris* species. Polymorphisms in nuclear rDNA (18S–ITS1–5.8S–ITS2–28S) further support their genetic distinctness. Several plastid haplotypes were detected within *I. ruthenica*, but none differentiated its varieties (var. *nana*, var. *brevituba*) or its close relative *I. uniflora*. Although no consistent

Поступило в редакцию 29.11.2025
Принято к публикации 11.12.2025

Submitted 29.11.2025
Accepted 11.12.2025

morphological differences were detected, we found compelling molecular evidence supporting the recognition of this lineage as a distinct species, which is formally described here as *I. cryptoruthenica*. Based on current data, its known range includes the Altai Mountain Country and northern China (Xinjiang).

Iris cryptoruthenica sp. nov. (Iridaceae): криптический вид морфотипа *Iris ruthenica*, выявленный баркодированием хлоропластной и рибосомальной ДНК и методами кариосистематики

П. М. Журбенко[1], К. А. Вильсон[6], В. И. Дорофеев[1], Т. В. Матвеева[4, 5], В. В. Коцеруба[1], В. С. Шнеер[1], Е. Д. Бадаева[2], М. В. Скапцов[3], А. И. Шмаков[3], А. В. Родионов[1, 4], Н. Б. Алексеева[1]

[1] *Ботанический институт им. В. Л. Комарова РАН, ул. Проф. Попова, д. 2, г. Санкт-Петербург, 197022, Россия*

[2] *Институт общей генетики им. Н. И. Вавилова РАН, ул. Губкина, д. 3, г. Москва, 119991, Россия*

[3] *Алтайский государственный университет, пр. Ленина, д. 61, г. Барнаул, 656049, Россия*

[4] *Санкт-Петербургский государственный университет, Университетская наб., д. 7, 9, г. Санкт-Петербург, 199034, Россия*

[5] *Всероссийский НИИ защиты растений, пр. Подбельского, д. 3, г. Санкт-Петербург – Пушкин, 196608, Россия*

[6] *Калифорнийский университет Беркли, 1001, Валлей Лайф Сайнс, № 2465, г. Беркли, Калифорния, 94720-2465, США*

Ключевые слова: ирис, криптический вид, покрытосеменные растения, размер генома, цитотипы.

Аннотация. *Iris ruthenica* – сибирский таёжно-степной вид, чья генетическая структура оставалась малоизученной. В ходе исследования *I. ruthenica* флоры Алтайской горной страны мы обнаружили криптический вид, морфологически неотличимый от *I. ruthenica* s. str., но отличающийся числом хромосом. Все изученные российские популяции *I. ruthenica* имеют $2n = 84$, тогда как криптический вид обладает $2n = 42$; данные проточной цитометрии показывают различие в размере генома (1C = 4,025 ± 0,110 pg против 1C = 2,135 ± 0,020 pg). Сравнительный анализ участков хлоропластной ДНК, охватывающих интервалы *atpB–accD* и *rpl2–matK* (включая гены *atpB*, *accD*, *psbA*, *rbcL*, *rpl2*, *rps19*, *matK* и *ycf1*) выявил, что генетическое расстояние между двумя линиями составляет около 0,5 %, что сопоставимо с расстоянием между некоторыми видами рода. Полиморфизм ядерной рДНК (18S–ITS1–5.8S–ITS2–28S) также подтверждает их генетическую обособленность. Внутри *I. ruthenica* на основании хлоропластной ДНК выявлено несколько гаплотипов, однако ни один из них не соотносится с разновидностями (var. *nana*, var. *brevituba*) или близкородственным видом *I. uniflora*. Несмотря на отсутствие диагностических морфологических различий, полученные молекулярные данные подтверждают эволюционную самостоятельность криптического вида, который мы описываем здесь как *I. cryptoruthenica*. Согласно имеющимся данным, его ареал включает Алтайскую горную страну и северные провинции Китая (Синьцзян).

Introduction

Iris L. are herbaceous, perennial geophytes with bulbs, tubers, or rhizomes and are distributed across the Northern Hemisphere. They share similar 3-merous flowers with petaloid tepals and petaloid blades of style. Their leaves are mostly unifacial although some groups such as *Iris* subgen. *Scorpiris* Spach have dorsiventral leaves. *Iris ruthenica* Ker Gawl. and its close relative *I. uniflora* Pall. ex Link are in *I.* subgen. *Limniris* (Tausch) Spach and the only members of *I.* ser. *Ruthenicae* (Diels) Lawrence (Mathew, 1997). These two species are relatively small plants with slender rhizomes, narrow grass-like leaves, and white, light blue, or violet flowers that are about 5 cm in diameter and lack sepal beards.

Not surprising given its wide geographical range, several infraspecific taxa have been named in *I. ruthenica*, including var. *albiflora* Bunge, subsp. *brevituba* (Maxim.) Doronkin, and var. *nana* Maxim. Each of these taxa was described based on relatively minute differences in morphology such as color, plant size, and floral tube length. The recognition of these taxa as distinct as well as *I. uniflora* when compared to *I. ruthenica* has been questioned (Mathew, 1997; Choi et al., 2022) suggesting that

the series may be monospecific. Alternatively, Zheng et al. (2017) found differences in leaf length and width between *I. ruthenica* and *I. uniflora* in addition to distributional differences and suggested that *I. uniflora* should remain segregated from *I. ruthenica*.

While examining the karyotypes of *I. ruthenica* in the Altai Mountain Country, we found evidence for two cytotypes. Plants from the vicinity of Artybash Village, the Republic of Altai of the Russian Federation had $2n = 42$, whereas other specimens of *I. ruthenica* from the Altai Territory showed $2n = 84$ (Zhurbenko et al., 2023). Since some cytotypes are known to represent cryptic species (Shneyer et al., 2018), it was of particular interest to compare the morphology of plants from the Artybash Village population with other specimens, determine their genome sizes, and analyze DNA barcodes by sequencing the most informative regions of the chloroplast genome as well as nuclear rDNA.

The goals of this study were to examine genetic, morphological, and distributional differences among plants from a significant portion of the range for *I. ruthenica* s. l. We provide evidence that the selected genetic features are reliable and sufficient to confirm the independent evolutionary trajectory of the lineage morphologically assignable to *I. ruthenica*. To clarify species boundaries and to facilitate future comparative and evolutionary research, a new species, *I. cryptoruthenica* is described here.

Materials and methods

Plant material

The study is based on both herbarium and living specimens of *I. ruthenica* s. l. and *I. uniflora*. Living specimens were collected by the authors during field expeditions and herbarium materials were selected from the V. L. Komarov Botanical Institute (LE, St. Petersburg) and Altai State University (ALTB, Barnaul) Herbaria. Complete chloroplast genome sequences available from NCBI under accessions MK593167, MK593169, OM037823, and OM037824, along with *I. ruthenica rbcL* gene sequences MT930336 and MT930337, were also used. In total, 65 samples were included in the molecular analyses: seven belonging to *I. uniflora*, one to *I. ruthenica* subsp. *brevituba*, five to *I. ruthenica* var. *nana*, eight to the *I. cryptoruthenica*, a new cryptic species described here, and the remainder to *I. ruthenica* s. str. The examined specimens originate from Romania, Kazakhstan, Mongolia, China, Republic of Korea, and Russian Federation (Novosibirsk Region, Altai Territory, Republic of Altai, Republic of Tuva, Irkutsk Region, Chita Region, Krasnoyarsk Territory, and Primorye Territory). Detailed information on sample provenance and the types of analyses conducted for each accession is provided in Supplementary Table S1. A map showing the collection sites of the studied samples is provided in Fig. 1.

Morphological examination

Morphological examination to identify potential diagnostic traits of the cryptic lineage was conducted on 50 herbarium specimens, including 40 of *I. ruthenica* and 10 of the *I. cryptoruthenica*, all collected in the Altai Territory. In addition, living plants from the same region (10 *I. ruthenica* and one *I. cryptoruthenica*) were examined in cultivation in the Iris Collection (Iridarium) of the Komarov Botanical Institute's Botanical Garden of Peter the Great. Both vegetative and reproductive organs were examined, including underground structures and parts of flowers. Observations were carried out visually and with the aid of a light microscope, without the preparation of anatomical sections. No anatomical, micromorphological, or statistical analyses were performed.

Chromosome counting and nuclear genome size estimation

For chromosome counting and nuclear genome size estimation, live specimens collected from the Altai Mountain Country were utilized (Supplementary Table S1). Chromosome counts were carried out on root meristem. Young roots were cut from potted plants, treated in 0.05 % colchicine at room temperature for 2 hours and fixed in ethanol – glacial acetic acid (3:1 v/v) for 1–2 weeks. The roots were stained in 2 % acetocarmine and squashed in a drop of acetic acid. Slides were examined on a Zeiss AxioImager D-1 epifluorescent microscope equipped with an AxioCam HRm black-and-white digital camera (Zeiss, Germany) and the selected metaphase cells were captured using software AxioVision, version 4.6.3. The facilities for chromosome analysis were provided by the N. I. Vavilov Institute of General Genetics, Russian Academy of Sciences.

Flow cytometry for nuclear genome size estimation was performed at Altai State University. Samples were chopped using a sharp razor blade in Tris-$MgCL_2$ buffer containing PI (50 μg/ml), RNase (50 μg/ml) supplemented with 2 mkl/ml 2-mercaptoethanol (Pfosser et al., 1995). The nuclear suspension was filtered through a nylon filter

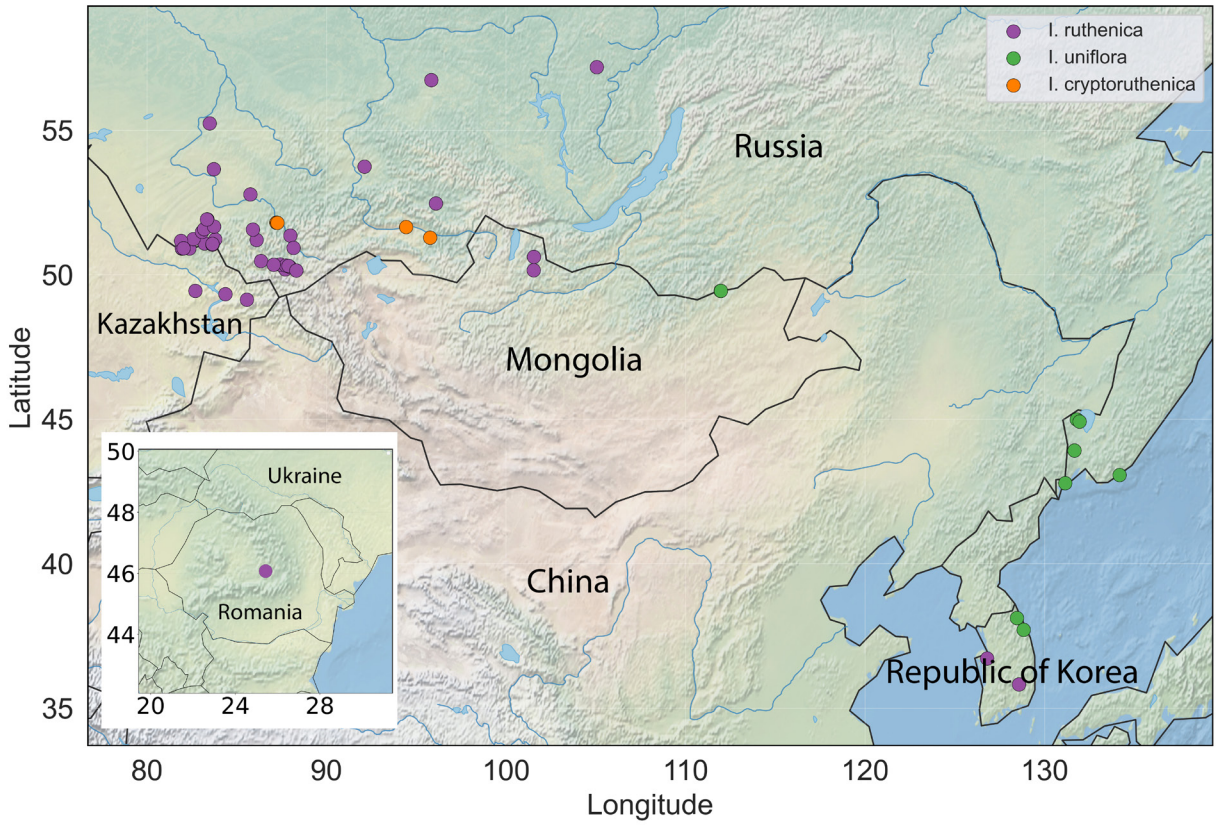

Fig. 1. Map showing collection localities of the studied samples, including *Iris ruthenica*, *I. uniflora*, and *I. cryptoruthenica*. Accessions from the Republic of Korea were obtained from NCBI.

with a pore size 30 μm. Analyses were performed on a Partec CyFlow PA (Sysmex Partec GmbH.) cytometer. *Allium fistulosum* L. (1C = 12.502 pg) was used as an internal standard (Skaptsov et al., 2024).

Chloroplast DNA sequencing and analysis

The analysis was conducted in two stages: an initial screening of specimens to identify divergent accessions, followed by sequencing of longer chloroplast genome regions in the selected accessions to extend sequence length and increase the number of informative sites. This strategy resulted in two datasets: (i) a main dataset (~ 1.7 kbp, Sanger sequencing) comprising 59 specimens, and (ii) an extended dataset (~ 7 kbp, NGS) generated for 10 divergent specimens from the first dataset. OneTaq® Hot Start DNA Polymerase (New England Biolabs, Ipswich, MA, USA; Cat. No. M0481) was used for PCR amplification. Primer sequences and annealing temperatures are provided in (Supplementary S2).

The main dataset was constructed from partial sequences of the *rbcL* and *ycf1* genes, together with the *petA–psbJ* intergenic spacer (~ 1.7 kbp in total). These sequences were obtained from 59 specimens at the Shared Core Facilities of the V. L. Komarov Botanical Institute. Not all specimens were successfully sequenced for every marker, resulting in some missing data (see Supplementary Table S1 for details). Sequencing chromatograms were processed in MEGA X (Kumar et al., 2018).

The extended dataset consisted of two chloroplast genome regions totaling ~ 7 kbp that were amplified by PCR and sequenced using next-generation sequencing (NGS) with paired-end 150 bp reads. These regions comprised (1) partial *atpB*, *atpB–rbcL*, *rbcL*, *rbcL–accD*, and partial *accD*; and (2) partial *rpl2*, *rpl2–rps19*, *rps19*, *rps19–psbA*, *psbA*, *psbA–matK*, and partial *matK*. For three additional specimens, only the *rpl2–matK* region was obtained. NGS reads were mapped to a reference genome using BWA-MEM (v0.7.17) (Li, 2013) and SAMtools (v1.17) (Danecek et al., 2021), with mapping visualized in IGV (Robinson, 2011). Variant calling was performed with bcftools 1.22 (Danecek et al., 2021), and FASTA sequences were aligned with MAFFT v.7 (Katoh, Standley, 2013) and manually curated.

The constructed datasets were further supplemented with GenBank accessions MT930337 and MT930336 (*I. ruthenica*, partial *rbcL* sequences), and sequence data for targeted markers that was

extracted from four complete chloroplast genome sequences available in GenBank: *I. ruthenica* (MK593167, OM037823) and *I. uniflora* (MK593169, OM037824). In addition, sequences of several other *Iris* species were incorporated for comparative purposes (accessions listed in Supplementary S2).

DNA alignment along with pairwise (p-) distance calculations for both datasets were conducted in MEGA X. A dataset with *I. ruthenica*, *I. uniflora* and nine outgroups from other series in *I.* subgen. *Limniris* was assembled in Geneious ver. 9.1.8 (Biomatters Ltd., Auckland, New Zealand). Maximum likelihood (ML) using RAxML (Stamatakis, 2014) and Bayesian inference (BI) using MrBayes (Ronquist et al., 2012) were performed to produce phylogenetic trees. ML analyses used the GTR model, partitions that were edge-linked, and 1000 bootstrap replicates (Felsenstein, 1985). BI analyses used four chains (one cold and three hot), and 3,000,000 generations with 3000 discarded trees. Model parameters were estimated during simulation. Branch support, posterior probabilities (PP) and bootstrap (BS) values, are shown above branches (PP/BS) with branches collapsed that have less than PP < 90 and BS < 50.

Ribosomal DNA library preparation and variant analysis

A two-step approach was used to characterise ITS1 sequence variation in *I. ruthenica*. In the first step, the entire ITS1 fragment of a representative specimen (Ru18) was sequenced on the Illumina MiSeq platform with 2 × 300 bp reads, providing complete coverage of the region and enabling recovery of intragenomic sequence variants. In the second step, these variants were incorporated into a reference sequence that was used for variant calling in a total of seven specimens, for which the ribosomal DNA region spanning 18S ITS1–5.8S–ITS2–26S was PCR-amplified and sequenced on the Illumina HiSeq platform with 2 × 150 bp paired-end reads.

Raw MiSeq reads were quality-filtered and denoised with the ZOTUs pipeline in USEARCH (Edgar, 2010), and variants represented by fewer than four reads were excluded. For reference construction, the 18S and 26S fragments were retrieved from GenBank (18S: JQ283937.1; 26S: JQ283879.1), 5.8S and ITS2 from GenBank (MT922613.1), whereas the ITS1 region was obtained from MiSeq data from sample Ru18. Because multiple ribotypes were detected in Ru18, a majority-rule consensus sequence was generated. HiSeq reads were then mapped to this reference using BWA-MEM (v0.7.17) and processed with SAMtools (v1.17). Low-confidence bases (Q < 20) were masked as "N" with JVarkit, and alignments were locally realigned with ABRA (v2.0) (Mose et al., 2019). SNPs and indels were called with GATK HaplotypeCaller (v4.3.0; van der Auwera, O'Connor, 2020). Resulting VCF files were parsed in Python with PyVCF (v0.6.7), and shared polymorphisms among individuals were visualised with UpSet plots (Lex et al., 2014). Pairwise Jaccard distances based on biallelic sites were subjected to PCA in scikit-bio (v0.5.9) (Rideout et al., 2025), and the first two principal components were plotted to summarise inter-individual variation.

Map Construction

Geographic maps were created using Python (v3.12) with the packages GeoPandas, Matplotlib, and Rasterio. Base layers of country borders and physical features (rivers and lakes) were obtained from the Natural Earth dataset (public domain; URL: https://www.naturalearthdata.com). Topographic shading was added using the Natural Earth shaded relief raster (NE2, 1:50 million). Maps of haplotype distribution were generated using the Python package folium (v0.20.0).

Results

Nuclear genome size estimation and chromosome counting

Two distinct ploidy levels were detected among the analysed specimens, indicating a cytogenetic differentiation between *I. ruthenica* and *I. cryptoruthenica*. Specimens assigned to *I. cryptoruthenica* (CrRu1–4, CrRu7–8), collected in the vicinity of the Artybash Village, the Republic of Altai, were diploid, with a genome size of 1C = 2.135 ± 0.020 pg; chromosome counting in specimen CrRu1 confirmed a complement of $2n = 42$ (Fig. 2A).

In contrast, accessions of the *I. ruthenica* from the Tretyakovsky (Ru11, Ru12, Ru16, Ru17, Ru18) and the Loktevsky (Ru30) districts of the Altai Territory were tetraploid, exhibiting a significantly larger genome size of 1C = 4.025 ± 0.110 pg; specimen Ru30 showed a chromosome number of $2n = 84$ (Fig. 2B). Detailed information on sample collection sites is provided in the Supplementary Table S1.

Chloroplast DNA sequencing and analysis

Phylogenetic hypotheses (Fig. 3) resolved *I. ruthenica* and *I. uniflora* as monophyletic (PP = 1, BS = 99) with two strongly supported clades and one strongly and one weakly supported subclades, respectively. Most populations of *I. ruthenica* and

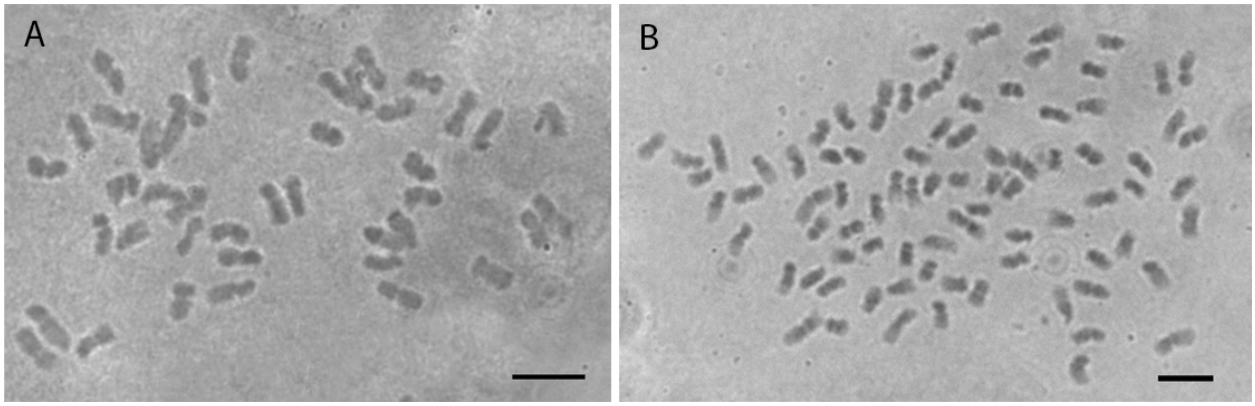

Fig. 2. Mitotic metaphases of (A) *Iris cryptoruthenica*, 2*n* = 42 and (B) *I. ruthenica*, 2*n* = 84. Scale bars = 10 μm.

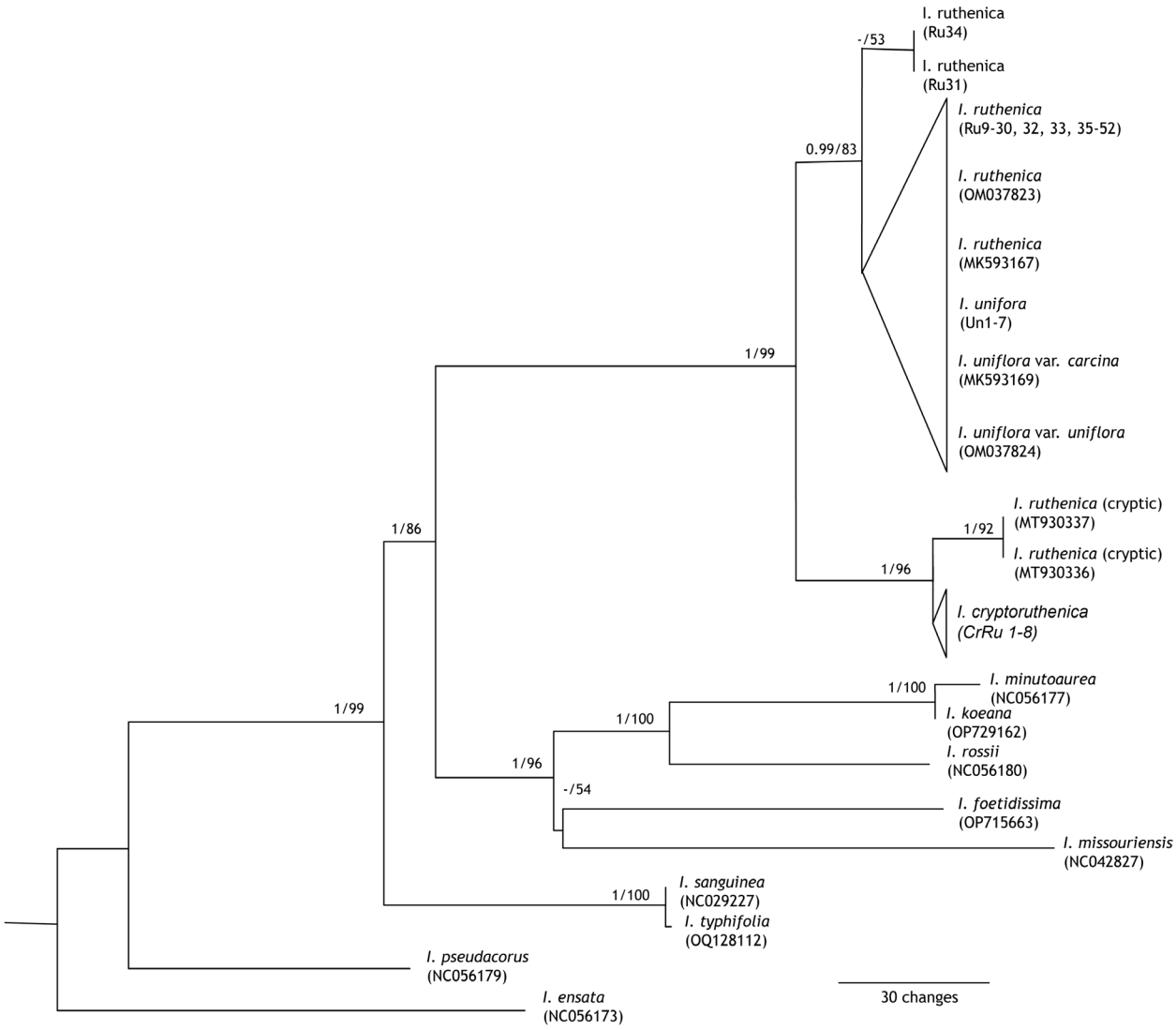

Fig. 3. Phylogenetic relationships among *Iris ruthenica* s. l., *I. uniflora*, and *I. cryptoruthenica* lineage inferred from chloroplast markers using Maximum Likelihood (RAxML) and Bayesian Inference (MrBayes). Support values (PP/BS) are shown above branches. The cryptic lineage (CrRu1–8, Russia; two accessions from Xinjiang, China) forms a strongly supported clade (PP = 1, BS = 96) sister to the *I. ruthenica* s. l. + *I. uniflora* clade. Branches with PP < 0.9 or BS < 50 are collapsed.

I. uniflora were resolved in a large clade (PP = 0.99, BS = 83) with no supported internal branches except one weakly supported subclade (PP < 90, BS = 53) with two populations of *I. ruthenica* from Russia, population 31 from the Kalman River area of the Altai Territory and population 34 from the Kurai Range of the Republic of Altai. Sister to the *I. ruthenica* + *I. uniflora* clade is a strongly supported clade (PP = 1, BS = 96) comprising eight samples of the *I. cryptoruthenica* (CrRu1-8) that were collected in Russia for this study and two accessions that were collected in Xinjiang, China and downloaded from GenBank. The Russian collections were from the area around the Artybash Village in the Republic of Altai and from two areas in the Republic of Tuva. The two Chinese collections comprise a strongly supported subclade (PP = 1, BS = 92). DNA sequence alignments are provided in Supplementary S3. Thus, phylogenetic analysis of chloroplast DNA revealed a clear separation between the *I. ruthenica* lineage and *I. cryptoruthenica*.

The main dataset. In the main dataset, *I. cryptoruthenica* was differentiated from *I. ruthenica* across all three loci by 17 SNPs and two indels. This lineage may also encompass the GenBank accessions MT930336 and MT930337, corresponding to partial *rbcL* sequences, which differed from the remaining accessions of *I. cryptoruthenica* by a single A/G polymorphism at position 39 of the gene. No synapomorphic substitutions specific to *I. uniflora* were identified, indicating its close affinity with *I. ruthenica*. Similarly, no genetic differences were detected in *I. ruthenica* subsp. *brevituba* and *I. ruthenica* var. *nana*. It should be noted that for *I. ruthenica* var. *nana*, sequence data were obtained only for the *ycf1* marker, and comparisons were therefore restricted to this locus. In contrast, within the *I. ruthenica* lineage, four distinct haplotypes were identified that were assigned to *I. ruthenica* subsp. *ruthenica*, each defined by SNPs or indels occurring in more than two accessions. Specifically, the indel haplotypes at *petA–psbJ*:530 (TATAA vs deletion) were found in 5 (TATAA) and 40 (deletion) samples; the SNP haplotypes at *petA–psbJ*:590 (T vs. A) occurred in 28 and 13 samples, respectively; and the indel haplotypes at *ycf1*:3634 (TCT vs. deletion) were detected in 18 and 30 samples respectively. Table 1 summarizes the diagnostic SNP and indel variation distinguishing the major haplotypes; coordinates are reported relative to the start of each gene or intergenic spacer. For clarity, a single representative accession from each lineage was included in the comparison. The table also shows haplotype variation within *I. ruthenica*. A full list of populations representing the haplotypes is provided in Supplementary Table S1, and the specific SNPs and indels for all samples are given in Supplementary Table S4.

The extended dataset. The ~7 kbp extended dataset was employed to provide a more complete estimate of genetic divergence between *I. cryptoruthenica* and *I. ruthenica* lineage. The dataset included one specimen (CrRu1) representing the cryptic lineage, whereas the remaining nine specimens belonged to *I. ruthenica* and *I. uniflora*. Pairwise p-distance values between the *I. cryptoruthenica* specimen CrRu1 and the other accessions ranged from 0.005 to 0.0058 (corresponding to 35–44 substitutions), whereas within the *I. ruthenica* lineage (including *I. uniflora*) the distances did not exceed 0.001 (≤ 7 substitutions).

To contextualize the degree of divergence observed between *I. ruthenica* and *I. cryptoruthenica*, we compared p-distances with those between selected *Iris* species. For this purpose, we selected species within several *Iris* sections that are genetically close to each other but nevertheless show clear morphological distinctness. For this purpose, the extended dataset was supplemented with homologous regions extracted from complete chloroplast genome sequences of additional *Iris* species from GenBank. The resulting p-distance values are presented as percentages (p-distance ×100) in Fig. 4, which also shows that pairwise genetic distances among species within the sections *Iris* and *Oncocyclus* (Siemssen) Baker, as well as within the subgenera *Pardanthopsis* (Hance) Baker and *Xiphium* (Miller) Spach, were lower than the divergence observed between *I. cryptoruthenica* and *I. ruthenica*. Importantly, a divergence value of 0.5–0.6 % was observed between species from different sections, for example, between *I. bloudowii* Ledeb. (sect. *Psammiris* (Spach) J. Taylor) and *I. imbricata* Lindl. (sect. *Iris*), as well as between *I. imbricata* (sect. *Iris*) and *I. atropurpurea* Baker (sect. *Oncocyclus*). In the latter case the genetic distance is even smaller than that between *I. cryptoruthenica* and *I. ruthenica*. Species of sect. *Limniris* Tausch displayed higher divergence, a pattern typical for this section where interspecific evolutionary distances are usually greater and correspond to a greater number of morphological differences among species.

rDNA sequencing and analysis

Analysis of the reference specimen Ru18, sequenced on the Illumina MiSeq platform with 2×300 bp reads, revealed seven distinct ITS1 ribotypes (Fig. 5A). The corresponding rDNA sequences are provided in Supplementary S3.

Table 1. Summary of nucleotide differences distinguishing *Iris cryptoruthenica* from the *I. ruthenica* lineage in the chloroplast markers *rbcL*, *ycf1*, and the *petA–psbJ* intergenic spacer

		rbcL				***petA–psbJ* spacer**											***ycf1***				
		304	311	531	606	50	79	91	131	141	150	387	502	530	590	591	3538	3634	3759	3879	3895
Iris ruthenica	Ru16	G	A	G	T	C	G	G	C	A	TAC	C	T	TAT AA	T	A	G	TCT	T	G	G
	Ru11	.	.	.	.	.	.	.	.	.	.	.	.	TATA ATA TAA	.	.	.	.	.	.	.
	Ru22	.	.	.	.	.	.	.	.	.	.	.	.	.	A	.	.	.	.	.	.
	Ru26	.	.	.	.	.	.	.	.	.	.	.	.	.	A	.	.	TCT TCT	.	.	.
Iris cryptoruthenica	CrRu1	A	T	A	C	T	T	T	T	G	TAC TAC	T	G	.	.	C	A	—	A	T	A

These ribotypes showed substantial sequence divergence from each other, indicating pronounced intragenomic heterogeneity within the rDNA array.

Sequencing of the ribosomal DNA region (18S–ITS1–5.8S–ITS2–26S) in a total of seven specimens using the Illumina HiSeq platform (2 × 150 bp paired-end reads) produced alignments to the reference with an average depth of ~ 4700×per site (see Supplementary S2). Variant calling identified 60 polymorphic positions across the dataset. Of these, 31 were located within ITS1, 19 within ITS2, 5 in 18S, and 5 in 26S, whereas the 5.8S gene was completely conserved. The distribution of polymorphisms across regions displayed a consistent pattern: specimens CrRu1 and CrRu6, representing *I. cryptoruthenica*, were differentiated from the other accessions by a distinct set of variants.

To summarise overall divergence, all variants (ribotypes) detected across the sequenced rDNA fragment were considered jointly. An intersection

			I. ruthenica Ru16	*I. cryptoruthenica* CrRu1	*I. uniflora*	*I. ensata*	*I. pseudacorus*	*I. setosa*	*I. foetidissima*	*I. tingitana*	*I. filifolia*	*I. xiphium*	*I. pskemensis*	*I. atropurpurea*	*I. paradoxa*	*I. germanica*	*I. imbricata*	*I. lutescens*	*I. bloudowii*	*I. flavissima*	*I. dichotoma*
Iris subg. *Limniris* sect. *Limniris*	ser. *Ruthenicae*	*I. ruthenica* Ru16																			
		I. cryptoruthenica CrRu1	0,50																		
		I. uniflora	0,07	0,55																	
	ser. *Laevigatae*	*I. ensata*	1,88	2,00	1,92																
		I. pseudacorus	1,95	2,03	2,01	1,06															
	ser. *Tripetalae*	*I. setosa*	1,96	2,04	1,99	1,09	1,04														
	ser. *Foetidissimae*	*I. foetidissima*	2,09	2,19	2,10	1,89	2,02	1,98													
Iris subg. *Xiphium*	*sect. Xiphium*	*I. tingitana*	2,38	2,41	2,40	2,16	2,31	2,27	1,01												
		I. filifolia	3,20	3,22	3,51	2,94	3,15	3,16	1,85	0,40											
		I. xiphium	3,60	3,62	3,62	3,37	3,53	3,47	2,20	0,40	0,29										
Iridodictium		*I. pskemensis*	2,21	2,29	2,23	1,84	2,10	2,09	0,81	0,92	1,64	1,92									
Iris subg. *Iris*	sect. *Oncocyclus*	*I. atropurpurea*	2,42	2,55	2,42	2,27	2,31	2,27	1,67	1,81	2,56	3,04	1,64								
		I. paradoxa	2,43	2,56	2,43	2,29	2,32	2,29	1,68	1,82	2,58	3,05	1,65	0,01							
	sect. *Iris*	*I. germanica*	2,27	2,43	2,30	2,23	2,13	2,17	1,67	1,84	2,62	3,04	1,65	0,57	0,58						
		I. imbricata	2,23	2,36	2,24	2,18	2,13	2,14	1,53	1,79	2,59	3,04	1,62	0,49	0,50	0,23					
		I. lutescens	2,28	2,41	2,28	2,23	2,15	2,20	1,59	1,84	2,66	3,10	1,68	0,55	0,56	0,29	0,06				
	sect. *Psammiris*	*I. bloudowii*	2,29	2,43	2,30	2,21	2,23	2,22	1,75	1,84	2,67	3,11	1,71	0,76	0,77	0,64	0,56	0,62			
		I. flavissima	2,35	2,49	2,39	2,32	2,31	2,32	1,80	1,93	2,78	3,20	1,80	0,81	0,83	0,67	0,57	0,63	0,14		
Iris subg. *Pardanthopsis*		*I. dichotoma*	2,19	2,29	2,19	1,97	2,00	2,04	1,54	1,69	2,45	2,89	1,56	0,83	0,84	0,74	0,69	0,74	0,86	0,94	
		I. domestica	2,19	2,29	2,19	2,00	2,03	2,07	1,55	1,73	2,51	2,94	1,60	0,84	0,86	0,76	0,72	0,76	0,87	0,96	0,10

Fig. 4. Pairwise genetic distances (p-distance ×100) among *Iris* species based on the extended dataset. Values ≤ 0.6 are indicated in orange and those ≤ 1.1 in green. Values are rounded to one decimal place.

plot (Fig. 5B) demonstrated that *I. cryptoruthenica* specimens (CrRu1 and CrRu6) shared 16 ribotypes not present in the other specimens. Conversely, 6 ribotypes were shared among all accessions except *I. cryptoruthenica*, whereas the remaining polymorphisms occurred in various combinations across individuals. Principal component analysis (PCA) based on all biallelic sites (Fig. 5C) further confirmed this separation: *I. cryptoruthenica* specimens clustered apart from the *I. ruthenica* and *I. uniflora*. Notably, specimen Ru13 also deviated from the remaining *I. ruthenica* accessions, highlighting variation in rDNA composition within the species.

Distribution

Specimens of *I. cryptoruthenica* (CrRu1–4, CrRu7–8) were collected in the Republic of Altai, in the vicinity of the Artybash Village near Lake Teletskoye, and in the Republic of Tuva (CrRu5 near the city of Kyzyl and CrRu6 near the village of Belbey). The NCBI accessions MT930337 and MT930336, which are nearly identical in their *rbcL* sequences to specimens CrRu1–8 (differing by a single nucleotide), likely also belong to this lineage. Unfortunately, the precise collection sites of these accessions are unknown. The NCBI annotation states that they were obtained within the framework of the project "DNA Barcoding Study of Desert Plants in Xinjiang, China." The Xinjiang province occupies a vast territory in northwestern China and shares a northern border with the Republic of Altai. The remaining specimens, including two from Romania, were assigned to *I. ruthenica*.

All other *I. ruthenica* and *I. uniflora* specimens, including those from Romania and Russia, as well as NCBI accessions from the Republic of Korea, are genetically very similar. Within this group, haplotypes differing by single substitutions or indels can be distinguished. Because the number of specimens sequenced varied among markers (Supplementary S1), distribution maps were constructed separately for each haplotype. Haplotypes: *petA–psbJ*:530 (TATAA vs deletion; Supplementary S5, Map 2), *petA–psbJ*:590 (T vs. A; Supplementary S5, Map 3), *ycf1*:3634 (TCT vs. deletion; Supplementary S5, Map 4).

Morphological examination

No reliable morphological characters distinguishing *I. cryptoruthenica* from *I. ruthenica* were identified. Particular attention was paid to the structure of the leaf margin, as this trait was highlighted as diagnostic in the study by Choi et al. (2022) for separating *I. ruthenica* (serrated leaf margins, hypostomatic leaves) from *I. uniflora* (entire leaf margins, amphistomatic leaves). In

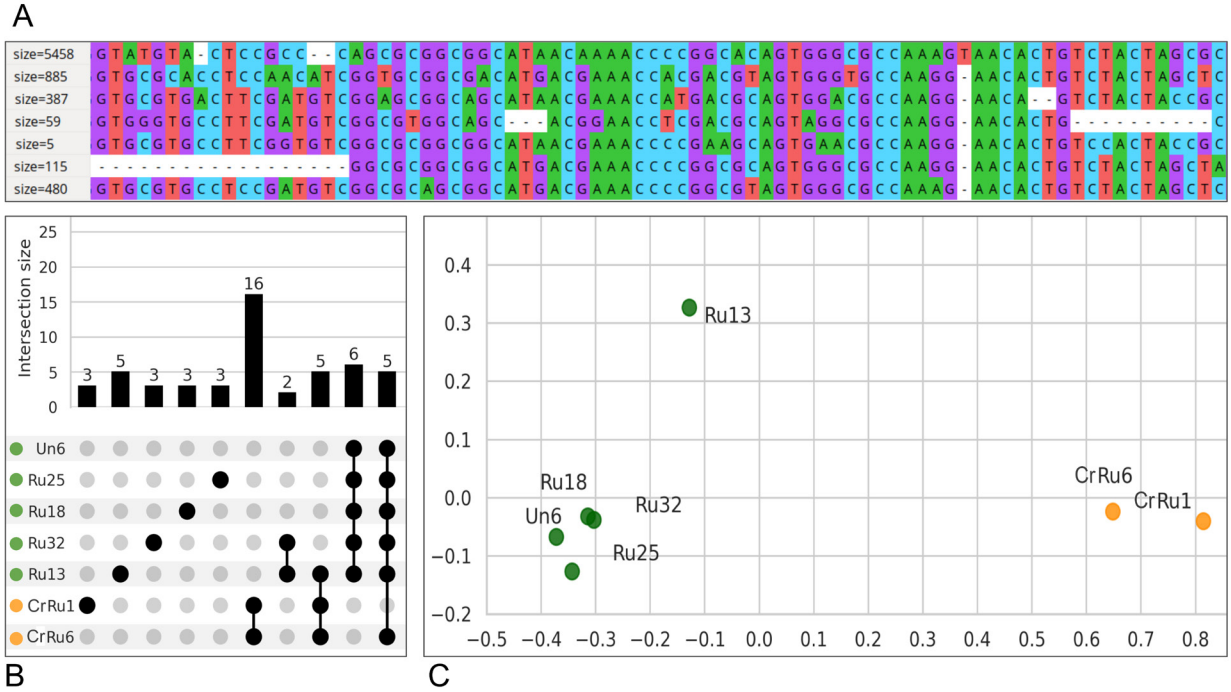

Fig. 5. A: ITS1 fragment variants (ribotypes) in *Iris ruthenica* (specimen Ru18). The parameter "size" indicates the number of reads supporting each variant. B: Intersection plot showing the distribution of ribotypes among specimens. Single intersections were removed. Orange circles represent *I. cryptoruthenica* specimens, and green circles represent *I. ruthenica*. C: Principal component analysis (PCA) based on a Jaccard distance matrix reflecting the number of shared ribotypes among specimens. Orange points denote *I. cryptoruthenica* specimens, and green points denote *I. ruthenica*.

our material, however, serrated leaf margins (see Supplementary S6) were observed in all specimens examined, including both *I. ruthenica* and *I. uniflora*.

Discussion

No genetic differentiation was detected either between *Iris uniflora* and *I. ruthenica* or among the varieties of *I. ruthenica*

In the "Flora of China" (Zhao et al., 2002), *I. ruthenica* is described as "...very variable and grades into *I. uniflora*." The authors also suggest that *I. ruthenica* subsp. *brevituba* and *I. ruthenica* var. *nana* do not merit recognition as separate taxa. In the "Checklist of Vascular Plants of Asian Russia" (Chepinoga et al., 2024), *I. ruthenica* subsp. *brevituba*, which occurs in the Altai-Yenisei Mountain-Hemiboreal Botanical Provinces of Asian Russia, is treated as distinct at the species level as *I. brevituba* (Maxim.) Vved. Mathew (1997) listed two varieties and one form under *I. ruthenica* in his monographic work on *Iris* but suggested that *I. ruthenica* might be considered as a species with several forms. Mathew (1997) also suggested that *I. uniflora*, where he listed two varieties, might be a variant of *I. ruthenica* but did not place any of these taxa in synonymy. He concluded that *I.* ser. *Ruthenicae* required additional research to determine if it was comprised of two species and several infraspecific taxa or one variable species. *Iris uniflora* similar to *I. ruthenica* has a wide distribution but does not extend into Eastern Europe. According to Alexeeva (2008), the distribution range of *I. uniflora* in Russia includes southern Eastern Siberia and Primorye, while outside Russia it occurs in China and the Republic of Korea. In the "Flora of China", *I. uniflora* is described as "...almost certainly merely a variety of *I. ruthenica*." *I. uniflora*, like *I. ruthenica*, appears to be highly morphologically variable. Probatova (2006, p. 501) characterized it as "an East Siberian-Far Eastern (primarily Amur-Korean) meadow-edge species, highly polymorphic." Based on their narrower and shorter leaves when compared to leaves of *I. ruthenica*, Zheng et al. (2017) recognized the species as distinct. They also noted that *I. uniflora* occupied a more xeric landscape than *I. ruthenica* and suggested that their leaf morphology might be related to habitat preferences. Choi et al. (2022) examined leaf, flower, and tepal micromorphology of plants from populations in the Republic of Korea and generated one plastome each of *I. ruthenica* and *I. uniflora* to determine differences between the two taxa. Results of their micromorphological studies found no clear differences between the two species except pollen sterility, with *I. uniflora* displaying greater sterility. They attributed this to its occurrence in colder regions in the Republic of Korea compared to the more widespread *I. ruthenica*. Although they found some genomic variation between the two species, they concluded that based on their results it was doubtful that the species can be recognized as distinct.

The results of our study confirm the results of Choi et al. (2022). We included multiple populations of *I. ruthenica* and *I. uniflora* from Russia, China, and the Republic of Korea in our study including several ones that represented infraspecific taxa. Plastid haplotype, rDNA, and plastid marker phylogenetic results indicate that the genetic differences between *I. ruthenica* and *I. uniflora* are minimal and do not exceed the range of haplotype variation observed within *I. ruthenica*. In addition, an examination of specimens gathered for this study did not find morphological differences that separate any of the populations except that some accessions considered *I. uniflora* had smaller leaves and the five accessions identified as *I. ruthenica* var. *nana* were slightly smaller than most populations surveyed.

Evidence for the recognition of the *Iris cryptoruthenica* as a distinct species

Cryptic species

Cryptic species have long been known, mostly comprising morphologically indistinguishable animal species that differ in behavioural traits (Darlington, 1940; Mayr, 1942). Soon after molecular methods began to be employed in systematics, there was an increasing number of reports identifying cryptic species, predominantly among a wide range of taxonomic groups in animals (Bickford et al., 2007; Kon et al., 2007; McLeod, 2010) and fungi (Bennet et al., 2011; McPherson et al., 2025). Cryptic species are also found among plants, although such finds are comparatively rare and occur in small number of lineages (see review by Shneyer, Kotseruba, 2015; Sokoloff et al., 2019; Heylen et al., 2021). However, many species with cytotypes of varying ploidy levels are known in plants (Müntzing, 1936; Shneyer et al., 2018). Sometimes, such intraspecies cytotypes have been found to exhibit other differentiating traits, leading to the classification of cytotypes as separate species (Judd et al., 2007; Flatscher et al., 2015; Punina et al., 2016). There have also been instances where new species were distinguished solely based on differences in ploidy and molecular markers (Eriksson et al., 2017).

The absence of morphological differentiation in cryptic species can arise for several evolutionary reasons, such as recent divergence, niche conservatism, or morphological convergence. These processes are less studied than morphological diversification and deserve more detailed investigation, as they may shed light on the mechanisms underlying speciation (Swift et al., 2016; Fišer et al., 2018; Struck et al., 2018).

In taxonomic practice, the ideal scenario is to apply an integrative approach that combines genetic, morphological, ecological, and geographical evidence (Dayrat, 2005; Padial et al., 2010). However, in cases involving cryptic species this approach may not work as intended, because morphological diagnostic traits cannot always be detected. Consequently, many morphologically cryptic lineages remain formally undescribed until such traits are found, even though these divergent traits may not exist or may be extremely difficult to recognize (Egea et al., 2016; Schüßler et al., 2024). This leads to a systematic bias: cryptic species are underrepresented in the taxonomic literature, which complicates the study of speciation involving morphological crypsis and contributes to an underestimation of biodiversity (Fišer et al., 2018; Hending et al., 2025). However, Fišer et al. (2018) emphasize that morphological crypsis may itself have clear evolutionary explanations, and that species hypotheses based solely on molecular evidence can be just as robust as those supported by full congruence among multiple independent data sources.

Phylogeny and genetic divergence

In the present study, we employed markers from both the chloroplast and nuclear genomes to ensure robustness of phylogenetic inference. In angiosperms, chloroplast genomes and ribosomal DNA represent among the most informative and frequently applied sources of data for reconstructing phylogenetic relationships (Soltis et al., 1999; Maia et al., 2014; Li et al., 2021; Dimitrov et al., 2023; Nafisi et al., 2023). Within *Iris*, chloroplast markers have long been used to resolve infrageneric relationships (Tillie et al., 2000; Wilson, 2004, 2011, 2013, 2016; Mavrodiev et al., 2016), while the ITS1 region of nuclear rDNA has been applied in studies of the Northern Hemisphere group of semi-aquatic species (Wheeler, Wilson, 2014). Several chloroplast loci applied here are well-established and phylogenetically informative, including *rbcL* (Chase, Albert, 1998; Goldblatt et al., 2008), *matK* (commonly used in *Iris* studies), the *petA–psbJ* intergenic spacer (Techaprasan et al., 2010; Maurya et al., 2025), and *ycf1* (Dong et al., 2015; Shen et al., 2020). Comparative analyses of nineteen *Iris* plastomes demonstrated that *ycf1* is among the three chloroplast markers exhibiting the highest congruence with full plastome phylogenies (Choi, Lee, 2024).

The *I. cryptoruthenica* lineage forms a well-supported clade that is sister to all other *I. ruthenica* and *I. uniflora* accessions. It exhibits substantial differentiation in chloroplast DNA, with divergence levels comparable to, or in some cases exceeding, those observed between recognized species within the genus *Iris*. In particular, the observed p-distance between *I. cryptoruthenica* and *I. ruthenica* is approximately 0.5 %, which is similar to or greater than some interspecific distances reported within *Iris* subg. *Xiphium* (sect. *Xiphium*), subg. *Iris* (sects. *Oncocyclus*, *Iris*, *Psammiris*), and subg. *Pardanthopsis*. Moreover, this divergence is about seven times greater than that between *I. ruthenica* and *I. uniflora*, or among haplotypes within *I. ruthenica*. Even acknowledging that substitution rates may vary among evolutionary lineages (Choi, Lee, 2024), the observed nucleotide divergence indicates pronounced genetic differentiation between *I. cryptoruthenica* and *I. ruthenica*.

Two Chinese accessions with available *rbcL* sequences (MT930337 and MT93033) are also resolved in the *I. cryptoruthenica* lineage but differ from the core *I. cryptoruthenica* haplotype by a single substitution. These samples can therefore be regarded as representing intraspecific variation within *I. cryptoruthenica*.

Nuclear rDNA provides congruent evidence. In *I. ruthenica*, the ITS1 region is represented by seven ribotypes, reflecting incomplete homogenization of rDNA repeats, a phenomenon widely documented in vascular plants (Belyakov et al., 2022; Efimov et al., 2024; Gnutikov et al., 2025). The presence of multiple ribotypes complicates the acquisition of clean Sanger sequences. Therefore, we applied next-generation sequencing (NGS) to obtain short reads covering the entire rDNA cluster for five samples of *I. ruthenica* and two of *I. cryptoruthenica*. Variant calling revealed polymorphic sites within each sample, and principal component analysis of the variant data showed a clear separation between the two taxa, fully consistent with the differentiation inferred from chloroplast markers. Taken together, chloroplast and nuclear datasets provide convergent evidence of deep genetic divergence, supporting the recognition of *I. cryptoruthenica* as evolutionarily distinct from *I. ruthenica*.

Chromosome number and genome size variation

Based on published data, two chromosome races can be recognized in *I. ruthenica*: a diploid race ($2n = 42$) and a tetraploid race ($2n = 84$). In the Republic of Korea, Choi et al. (2020) examined nine populations and reported a uniform chromosome number of $2n = 42$, with genome size estimates ranging from 2.39 to 2.45 pg/1C. Similarly, three populations studied in China (Shen et al., 2007) also showed the diploid number ($2n = 42$). In contrast, all Russian accessions examined to date, collected in Central and Southern Siberia (Krasnoyarsk Territory (Stepanov, Muratova, 1995), Irkutsk Region (Chepinoga et al., 2010), Republics of Buryatia, Tuva, and Altai (Doronkin, Krasnikov, 1984)), were tetraploid with $2n = 84$. Chromosome counts of $2n \approx 80$ have also been reported by other authors for specimens collected in the Republic of Altai (Krivenko et al., 2013, 2017).

Descriptions of chromosome numbers in *I. uniflora* are notably variable. In the Republic of Korea, three populations examined by Choi et al. (2020) were diploid ($2n = 42$), with genome sizes ranging between 2.44 and 2.48 pg/1C. In Russia, Doronkin and Krasnikov (1984) reported $2n = 42$ for populations of *I. uniflora* in the Chita Region. In the Primorye Territory, however, considerable cytogenetic variation has been documented. While most published chromosome counts indicate $2n = 48$ (Shatokhina, 2006; Probatova et al., 2012a, b, 2015), lower chromosome numbers of $2n = 32$ were also documented by Probatova (Probatova et al., 2008). Probatova (2006) also noted earlier reports of $2n = 16$ from the Rudnaya River basin near Dalnegorsk and $2n = 48$ from Popov Island (Agapova et al., 1990), emphasizing that the detection of a tetraploid race with $2n = 32$ further illustrates the remarkable cytogenetic diversity reported under *I. uniflora*. We consider that plants identified as *I. uniflora* with $2n = 42$ may possibly include representatives of *I. cryptoruthenica*, although targeted molecular and cytogenetic analyses are needed to verify this. Plants with $2n = 32$ and $2n = 16$ likewise require further study and may represent other, potentially undescribed species of *Iris*.

Estimates of genome size based on flow cytometry can provide additional information on cytological diversity. The tetraploid *I. ruthenica* lineage ($2n = 84$) has a haploid genome size (1C) of 4.025 ± 0.110 pg, corresponding to a monoploid genome size (Cx) of 2.013 ± 0.055 pg. This shows a marked reduction in DNA content relative to the expected additive value of diploids, implying post-polyploidization DNA loss. Such genome downsizing is commonly observed in angiosperms (Rodionov et al., 2019) following polyploidization and likely reflects large-scale elimination of repetitive sequences and genome restructuring. Genome size estimates for the diploid *I. cryptoruthenica* ($2n = 42$; $1C = 2.135 \pm 0.020$ pg) and diploid populations of some *I. ruthenica* ($2n = 42$; 1C = 2.39–2.45 pg, according to Choi et al., 2020) differ markedly despite having an identical chromosome number. Genome size is one of the traits that has been shown to reliably distinguish closely related species (Ekrt et al., 2010; Prančl et al., 2014). The ~ 12 % higher 1C value in *I. ruthenica* suggests substantial differences in the amount of repetitive DNA or indicates large-scale structural rearrangements in the genome (Pellicer et al., 2018) that occurred after divergence, which supports the interpretation of *I. cryptoruthenica* as a distinct lineage separate from *I. ruthenica*.

Morphological analysis

Examination of both living and herbarium specimens of *I. cryptoruthenica* has not yet revealed any reliable morphological characters suitable for distinguishing it from related taxa. Given the high level of intraspecific morphological variation in *I. ruthenica* (Zhao et al., 2002), a more extensive statistical analysis based on a larger sample size may be required to detect potentially morphological differences between *I. cryptoruthenica* and *I. ruthenica*. The inability to identify clear morphological diagnostic traits in cryptic species has been reported previously in animals. For example, Egea et al. (2016) noted that morphological examination of 20 quantitative traits in the sea urchin *Echinocardium cordatum* s. l. revealed no single diagnostic character; however, consistent differences among cryptic species emerged only with detailed multivariate analysis. Similarly, in another study examining the insect *Encyrtus sasakii* s. l., comprehensive morphometric analyses revealed numerous differences between the taxa, yet none of them could be considered reliable for species diagnosis. Consequently, those cryptic species were formally described solely on the basis of differences in DNA sequences (Wang et al., 2016).

Geographical distribution and ecological characteristics

Currently, *I. cryptoruthenica* is known from only three localities. The first is in the Republic of Altai, in the vicinity of the Artybash Village near Teletskoye Lake, where the species was found at the edge of a mixed forest and in rock crevices. Two

additional localities occur situated in the Republic of Tuva, one near the city of Kyzyl and another near the village of Belbey, where plants were collected in a birch forest with a well-developed *Iris* ground cover. For two accessions from China assigned to the *I. cryptoruthenica* lineage in NCBI, only the province Xinjiang is known, without precise locality data. Based on these records, *I. cryptoruthenica* appears to occur within the general distribution range and ecological amplitude of *I. ruthenica*, inhabiting similar habitats at elevations from approximately 400 m (Republic of Altai) to 700 m a. s. l. (Republic of Tuva). Unfortunately, the available data are insufficient to determine any consistent ecological differences between *I. cryptoruthenica* and *I. ruthenica*.

Hypotheses explaining morphological crypsis

Cases where species exhibit strong genetic divergence without corresponding morphological differentiation are well documented and can have robust biological explanations. Fišer et al. (2018) outlined three non-mutually exclusive hypotheses to explain this phenomenon. The recent divergence hypothesis proposes that insufficient time has passed since lineage separation for diagnostic morphological traits to evolve. Slow morphological evolution may result from selectively neutral traits, large effective population size, and high ancestral polymorphism (Egea et al., 2016). The phylogenetic niche conservatism (or morphological stasis) hypothesis attributes morphological similarity to constrained genetic variation at adaptive loci and stabilizing selection maintaining an ancestral phenotype (Wiens et al., 2010). Such stasis can persist over long evolutionary timescales; for instance, two morphologically indistinguishable *Stygocapitella* species diverged approximately 140 Mya (Cerca et al., 2020). Finally, the morphological convergence hypothesis suggests that similar morphologies may evolve independently under comparable selective pressures (Stayton, 2006; Bravo et al., 2014).

To evaluate which of these hypotheses may best explain the case of *I. ruthenica*, we examined its morphology, ecology, and distribution range (Supplementary S7). *I. ruthenica* inhabits a wide spectrum of ecotopes, including coniferous and mixed forests, forest edges, dry mixed-grass and shrubby meadows, steppes, and alpine low-grass habitats, occurring at elevations from 400 up to 2500 m a. s. l. According to Tayier et al. (2024), the species grows on slopes of various exposures (N, SE, and SW) that differ in light intensity, temperature, and vegetation cover. It exhibits a mixed mating system, capable of both self- and cross-pollination, and demonstrates high phenotypic plasticity in phenology, clonal density, and shoot morphology. These traits indicate that *I. ruthenica* behaves as an ecological generalist with broad environmental tolerance and no signs of adaptive morphological radiation. *Iris ruthenica* is distributed across the boreal part of Asia, occurring from the taiga subzone to temperate steppe regions, and occupies an extensive range. Within its habitats, *I. ruthenica* often forms dense clonal patches and can locally dominate the herb layer, suggesting large effective population sizes and, consequently, a strong buffering effect of stabilizing selection. Based on current evidence, morphological convergence appears unlikely, as both lineages are assumed to derive from a common ancestor, and their morphological similarity is better interpreted as the retention of an ancestral phenotype rather than divergence followed by independent adaptation. Although recent divergence cannot be entirely ruled out, the magnitude of molecular differentiation comparable to that between morphologically distinct species suggests a longer evolutionary separation. It is therefore likely that the observed morphological crypsis reflects a combination of processes, with long-term morphological stasis under stabilizing selection within a broad ecological niche playing the predominant role.

Molecular basis for species recognition

Molecular markers are widely used for phylogenetic reconstruction across the Tree of Life (APG IV, 2016; Laumer et al., 2019; He et al., 2024; Zuntini et al., 2024). As a result, contemporary eukaryotic phylogenies are derived predominantly from molecular datasets (Burki et al., 2020). Within the framework of the evolutionary species concept (Simpson, 1951; Wiley, 1978; de Queiroz, 2007), molecular evidence therefore constitutes a legitimate and widely accepted basis for recognizing independently evolving lineages.

Although species descriptions in plants have traditionally relied on morphological traits, molecular data are increasingly integrated into taxonomic practice. The combined use of molecular and morphological evidence is now routine in many major organismal groups, including archaea, bacteria, chordates, and fungi (Ziegler et al., 2025).

Nevertheless, only about 14 % of newly described plant species incorporate molecular evidence, indicating that plant taxonomy lags behind broader systematic practice in this respect.

Importantly, current nomenclatural codes do not prohibit the use of DNA characters as the sole basis for species delimitation. Formal DNA-only descriptions have been published in fungi (Brown et al., 2013; Onut-Brännström et al., 2018; Bustamante et al., 2019), animals (Edgecombe, Giribet, 2008; Harvey et al., 2008; Halt et al., 2009; Cook et al., 2010; Strand, Sundberg, 2011; Jörger, Schrödl, 2013; Clouse, Wheeler, 2014; Murphy et al., 2015; Renner, 2016; Wang et al., 2016; Delić et al., 2017), and algae (Irisarri et al., 2021; Martynenko et al., 2022). Cook et al. (2010) explicitly stated that there is no compelling reason to exclude DNA-only descriptions or require morphological corroboration, emphasizing instead the scientific soundness of the taxonomic conclusion.

In this context, the combined evidence from chloroplast DNA, nuclear rDNA, and genome size (1C) consistently resolves *I. cryptoruthenica* as distinct from *I. ruthenica*. This congruence across independent molecular datasets warrants its recognition as a species. As diagnostic characters, we report the nucleotide substitutions identified in chloroplast DNA alignments between *I. cryptoruthenica* and *I. ruthenica*, following accepted taxonomic practice (Jörger, Schrödl, 2013; Renner, 2016).

Description of new species

Iris cryptoruthenica P. Zhurb., **sp. nov.**

Holotype (designated here): "Russian Federation, Republic of Altai, vicinity of Artybash village, forest edge, 51°48'02.2"N, 87°12'52.1"E, elev. 430 m a. s. l. 26 V 2018. leg. P. M. Zhurbenko 20181" (LE 01228640!). Note: originally identified as *I. ruthenica*.

Paratypes (originally identified as *I. ruthenica*): "Russian Federation, Republic of Tuva, Western Sayan, Usinsky Tract, 32 km from Kyzyl city, [51°39'N, 94°26'E]. 6 VIII 1959. leg. P. K. Krasilnikov, G. L. Semidel, P. D. Sokolov, det. P. K. Krasilnikov" (LE 01082929!); "Russian Federation, Republic of Tuva, Kaa-Khem District, vicinity of Belbey village, birch forest with *Iris* cover, [51°17'N, 95°46'E]. 28 VII 1975. leg. I. M. Krasnoborov, S. Ligus 1096" (LE 01082931!).

Diagnosis. Differs from *I. ruthenica* by substitutions in three chloroplast genome regions, relative to the reference chloroplast genome (NCBI accession NC_056181.1):

rbcL: positions 304 (G to A), 311 (A to T), 531 (G to A), 606 (T to C);

petA–psbJ spacer: positions 50 (C to T), 79 (G to T), 91 (G to T), 131 (C to T), 141 (A to G), 387 (C to T), 502 (T to G), 591 (A to C);

ycf1: positions 3538 (G to A), 3759 (T to A), 3879 (G to T), 3895 (G to A).

Description. Perennial rhizomatous herb forming small, dense tufts. Rhizomes slender, cord-like, branching, covered with grayish remnants of leaf sheaths. Leaves linear, soft, and narrow (0.4–0.6 cm wide, 20–30 cm long), arranged distichously, straight or slightly curved. Flowering stems 10–12 cm tall, with 2–3 inflated green spathes enclosing a single flower. Flowers fragrant, violet-blue to pale blue, the perianth with a short tube (1–1.2 cm) and six differentiated floral tepals: three outer (falls) 4 cm long and 0.8–1 cm wide, deflexed, with a whitish-yellow patch marked by blue lines; and three inner tepals (standards) narrower, erect, without markings. Style tribranches (trilobe) petaloid, 3.5–4 cm long, every one lobe deeply bifid at the apex, arching over the stamens. Capsule nearly spherical (12–15 mm), dehiscing along the midrib of each locule. Seeds brown, angular or pyramidally faceted, with faint arilloid folds. Flowering in May – June.

Etymology. The epithet reflects a hidden genetic difference from the morphologically similar *I. ruthenica*.

Acknowledgements

This study, including the cytogenetic and molecular analyses, was conducted as part of the research project "Molecular Phylogenetic Studies and Karyosystematics of Flowering Plants", state registration number 124020100136-0 and was carried out using the equipment of the Core Facilities Center "Cell and Molecular Technologies in Plant Science" at the Komarov Botanical Institute RAS (St. Petersburg, Russia).

Collection of plant material and genome size estimation by flow cytometry were supported by the State Assignment of Altai State University (project FZMW-2023-0008).

The American Iris Society Foundation supported this project through a travel grant to PMZ to train in DNA extraction methods in C. A. Wilson's laboratory at the University of California, Berkeley.

REFERENCES / ЛИТЕРАТУРА

Agapova N. D., Arkharova K. B., Vakhtina L. I., Zemskova E. A., Tarvis L. V. 1990. *Chisla khromosom tsvetkovykh rasteniy flory SSSR*: *Aceraceae – Menyanthaceae* [*Chromosome numbers of flowering plants of the USSR flora*: *Aceraceae –*

Menyanthaceae]. Leningrad: Nauka. 509 pp. [In Russian] (***Агапова Н. Д., Архарова К. Б., Вахтина Л. И., Земскова Е. А., Тарвис Л. В.*** Числа хромосом цветковых растений флоры СССР: Aceraceae – Menyanthaceae. Л.: Наука, 1990. 509 с.).

Alexeeva N. 2008. Genus *Iris* L. (Iridaceae) in Russia. *Turczaninowia* 11, 2: 5–68. [In Russian] (***Алексеева Н. Б.*** Род *Iris* L. (Iridaceae) в России // Turczaninowia, 2008. Т. 11, № 2. С. 5–68).

APG (*The Angiosperm Phylogeny Group*). 2016. An update of the APG classification for the orders and families of flowering plants: APG IV. *Bot. J. Linnean Soc.* 181(1): 1–20. https://doi.org/10.1111/boj.12385

Belyakov E. A., Mikhaylova Y. V., Machs E. M., Zhurbenko P. M., Rodionov A. V. 2022. Hybridization and diversity of aquatic macrophyte *Sparganium* L. (Typhaceae) as revealed by high-throughput nrDNA sequencing. *Sci. Rep*. 12: 21610. https://doi.org/10.1038/s41598-022-25954-0

Bennett C., Aime M. C., Newcombe G. 2011. Molecular and pathogenic variation within *Melampsora* on *Salix* in western North America reveals numerous cryptic species. *Mycologia* 103: 1004–1018. https://doi.org/10.3852/10-289

Bickford D., Lohman D. J., Sodhi N. S., Ng P. K. L., Meier R., Winker K., Ingram K. K., Das I. 2007. Cryptic species as a window on diversity and conservation. *Trends Ecol. Evol*. 22: 148–155. https://doi.org/10.1016/j.tree.2006.11.004

Bravo G. A., Remsen J. V. Jr., Brumfield R. T. 2014. Adaptive processes drive ecomorphological convergent evolution in antwrens (Thamnophilidae). *Evolution* 68(10): 2757–2774. https://doi.org/10.1111/evo.12506

Brown E. M., McTaggart L. R., Zhang S. X., Low D. E., Stevens D. A., Richardson S. E. 2013. A cryptic species *Blastomyces gilchristii* sp. nov. within *Blastomyces dermatitidis*. *PLOS ONE* 8(3): e59237. https://doi.org/10.1371/journal.pone.0059237

Burki F., Roger A. J., Brown M. W., Simpson A. G. B. 2020. The new tree of eukaryotes. *Trends Ecol. Evol*. 35(1): 43–55. https://doi.org/10.1016/j.tree.2019.08.008

Bustamante D. E., Oliva M., Leiva S., Mendoza J. E., Bobadilla L., Angulo G., Calderon M. S. 2019. Phylogeny and species delimitations in *Beauveria*, including *B. peruviensis* sp. nov. *MycoKeys* 58: 47–68. https://doi.org/10.3897/mycokeys.58.35764

Cerca J., Meyer C., Stateczny D., Siemon D., Wegbrod J., Purschke G., Dimitrov D., Struck T. H. 2020. Deceleration of morphological evolution in a cryptic species complex and its link to paleontological stasis. *Evolution* 74(1): 116–131. https://doi.org/10.1111/evo.13884

Chase M. W., Albert V. A. 1998. A perspective on the contribution of plastid *rbcL* to angiosperm phylogenetics. In: *Molecular Systematics of Plants* II. Boston: Springer. Pp. 488–507. https://doi.org/10.1007/978-1-4615-5419-6_17

Chepinoga V. V., Barkalov V. Yu., Ebel A. L., Knyazev M. S., Baikov K. S., Bobrov A. A., et al. 2024. Checklist of vascular plants of Asian Russia. *Bot. Pacifica*. 13, S3: 3–310. https://doi.org/10.17581/bp.2024.13S01

Chepinoga V. V., Gnutikov A. A., Enushchenko I. V. 2010. In: K. Marhold (ed.). IAPT/IOPB chromosome data 9. *Taxon* 59(4): 1298–1299. https://doi.org/10.1002/tax.594047

Choi B., Park I., So S., Myeong H. H., Ryu J., Ahn Y. E., Shim K. C., Song J. H., Jang T. S. 2022. Comparative analysis of two Korean irises (*Iris ruthenica* and *I. uniflora*, Iridaceae) based on plastome sequencing and micromorphology. *Sci. Rep*. 12: 9424. https://doi.org/10.1038/s41598-022-13528-z

Choi B., Weiss-Schneeweiss H., Temsch E. M., So S., Myeong H.-H., Jang T.-S. 2020. Genome size and chromosome number evolution in Korean *Iris* L. species (Iridaceae). *Plants* 9: 1284. https://doi.org/10.3390/plants9101284

Choi T. Y., Lee S. R. 2024. Complete plastid genome of *Iris orchioides* and comparative analysis with 19 *Iris* plastomes. *PLOS ONE* 19(4): e0301346. https://doi.org/10.1371/journal.pone.0301346

Clouse R. M., Wheeler W. C. 2014. Two cryptic species of *Metasiro* from South Carolina, USA. *Zootaxa* 3814(2): 177–201. https://doi.org/10.11646/zootaxa.3814.2.2

Cook L. G., Edwards R. D., Crisp M. D., Hardy N. B. 2010. Need morphology always be required for new species descriptions? *Invertebr. Syst.* 24(3): 322–326. https://doi.org/10.1071/IS10011

Danecek P., Bonfield J. K., Liddle J., Marshall J., Ohan V., Pollard M. O., Whitwham A., Keane T., McCarthy S. A., Davies R. M., Li H. 2021. Twelve years of SAMtools and BCFtools. *GigaScience* 10(2): giab008. https://doi.org/10.1093/gigascience/giab008

Darlington C. D. 1940. Taxonomic species and genetic systems. In: J. S. Huxley (ed.). *The New Systematics*. Oxford: University Press. Pp. 137–160.

Dayrat B. 2005. Towards integrative taxonomy. *Biol. J. Linn. Soc*. 85(3): 407–417. https://doi.org/10.1111/j.1095-8312.2005.00503.x

Delić T., Trontelj P., Rendoš M., Fišer C. 2017. The importance of naming cryptic species and the conservation of endemic subterranean amphipods. *Sci. Rep*. 7: 3391. https://doi.org/10.1038/s41598-017-02938-z

de Queiroz K. 2007. Species concepts and species delimitation. *Syst. Biol*. 56(6): 879–886. https://doi.org/10.1080/10635150701701083

Dimitrov D., Xu X., Su X., Shrestha N., Liu Y., Kennedy J. D. et al. 2023. Diversification of flowering plants in space and time. *Nat. Commun*.14: 7609. https://doi.org/10.1038/s41467-023-43396-8

Dong W., Xu C., Li C., Sun J., Zuo Y., Shi S., Cheng T., Guo J., Zhou S. 2015. *ycf1*, the most promising plastid DNA barcode of land plants. *Sci. Rep*. 5: 8348. https://doi.org/10.1038/srep08348

Doronkin V. M., Krasnikov A. A. 1984. Cytotaxonomic studies in some Siberian species of the genus *Iris* (Iridaceae). *Bot. Zhurn*. 65(5): 683–685. [In Russian] (***Доронкин В. М., Красников А. А.*** Цитотаксономические исследования некоторых сибирских видов рода *Iris* (Iridaceae) // Бот. журн., 1984. Т. 65, № 5. С. 683–685).

Edgar R. C. 2010. Search and clustering orders of magnitude faster than BLAST. *Bioinformatics* 26(19): 2460–2461. https://doi.org/10.1093/bioinformatics/btq461 (USEARCH and UCLUST algorithms)

Edgecombe G. D., Giribet G. 2008. A New Zealand species of the centipede order Craterostigmomorpha corroborated by molecular evidence. *Invertebr. Syst*. 22(1): 1–15. https://doi.org/10.1071/IS07036

Efimov P., Domashkina V., Machs E., Zhurbenko P. 2024. Evaluation of intragenomic polymorphism of ribosomal DNA ITS1 region in *Taraxacum* by targeted NGS sequencing. *Turczaninowia* 27, 3: 97–109. https://doi.org/10.14258/turczaninowia.27.3.10

Egea E., David B., Choné T., Laurin B., Féral J. P., Chenuil A. 2016. Morphological and genetic analyses reveal a cryptic species complex in *Echinocardium cordatum* and rule out stabilizing selection. *Mol. Phylogenet. Evol*. 94(Part A): 207–220. https://doi.org/10.1016/j.ympev.2015.07.023

Ekrt L., Holubová R., Trávníček P., Suda J. 2010. Species boundaries and frequency of hybridization in the *Dryopteris carthusiana* complex: a taxonomic puzzle resolved using genome size data. *Am. J. Bot*. 97: 1208–1219. https://doi.org/10.3732/ajb.0900206

Eriksson J. S., Blanco-Pastor J. L., Sousa F. D., Bertrand Y. J. K., Pfeil B. E. 2017. A cryptic species produced by autopolyploidy and subsequent introgression involving *Medicago prostrata* (Fabaceae). *Mol. Phylogenet. Evol*. 107: 367–381. https://doi.org/10.1016/j.ympev.2016.11.020

Felsenstein J. 1985. Confidence limits on phylogenies: An approach using the bootstrap. *Evolution* 39: 783–791.

Fišer C., Robinson C. T., Malard F. 2018. Cryptic species as a window into the paradigm shift of the species concept. *Mol. Ecol*. 27: 613–635. https://doi.org/10.1111/mec.14486

Flatscher R., García P. E., Hülber K., Sonnleitner M., Winkler M., Saukel J., Schneeweiss G. M., Schönswetter P. 2015. Underestimated diversity in one of the world's best studied mountain ranges: The polyploid complex of *Senecio carniolicus* (Asteraceae) contains four species in the European Alps. *Phytotaxa* 213(1): 1–21. https://doi.org/10.11646/phytotaxa.213.1.1

Goldblatt P., Rodriguez A., Powell M., Davies J., Manning J., Bank M., Vincent S. 2008. Iridaceae 'Out of Australasia'? Phylogeny, biogeography, and divergence time based on plastid DNA Sequences. *Syst. Bot*. 33(3): 495–508. https://doi.org/10.1600/036364408785679806

Gnutikov A. A., Nosov N. N., Loskutov I. G., Rodionov A. V., Shneyer V. S. 2025. Participation of wild species genus *Avena* L. (Poaceae) of different ploidy in the origin of cultivated species according to data on intragenomic polymorphism of the ITS1-5.8S rRNA region. *Plants* (Basel) 14(10): 1550. https://doi.org/10.3390/plants14101550

Halt M. N., Kupriyanova E. K., Cooper S. J. B., Rouse G. W. 2009. Naming species with no morphological indicators: species status of *Galeolaria caespitosa* (Annelida: Serpulidae) inferred from nuclear and mitochondrial gene sequences and morphology. *Invertebr. Syst*. 23(3): 205–222. https://doi.org/10.1071/IS09003

Harvey M. S., Berry O., Edward K. L., Humphreys G. 2008. Molecular and morphological systematics of hypogean schizomids (Schizomida: Hubbardiidae) in semiarid Australia. *Invertebr. Syst*. 22(2): 167–194. https://doi.org/10.1071/IS07026

He M.Q., Cao B., Liu F., Boekhout T., Denchev T., Schoutteten N. et al. 2024. Phylogenomics, divergence times and notes of orders in Basidiomycota. *Fungal Divers*. 26: 127–406. https://doi.org/10.1007/s13225-024-00535-w

Hending D. 2025. Cryptic species conservation: a review. *Biol. Rev*. 100: 258–274. https://doi.org/10.1111/brv.13139

Heylen O. C. G., Debortoli N., Marescaux J., Olofsson J. K. 2021. A Revised phylogeny of the *Mentha spicata* clade reveals cryptic species. *Plants* 10: 819. https://doi.org/10.3390/plants10040819

Irisarri I., Darienko T., Pröschold T. Fürst-Jansen J. M. R., Jamy M., de Vries J. 2021. Unexpected cryptic species among streptophyte algae most distant to land plants. *Proc. Biol. Sci*. 288(1963): 20212168. https://doi.org/10.1098/rspb.2021.2168

Jörger K. M., Schrödl M. 2013. How to describe a cryptic species? *Front. zool*. 10(1): 59. https://doi.org/10.1186/1742-9994-10-59

Judd W. S, Soltis D. E., Soltis P. S, Iontas G. 2007. *Tolmiea diplomenziesii*: a new species from the Pacific Northwest and the diploid sister taxon of the autotetraploid *T. menziesii* (Saxifragaceae). *Brittonia* 59(3): 217–225. https://doi.org/10.1663/0007-196X(2007)59[217:TDANSF]2.0.CO;2

Katoh K., Standley D. M. 2013. MAFFT multiple sequence alignment software version 7: improvements in performance and usability. *Mol. Biol. Evol*. 30(4): 772–780. https://doi.org/10.1093/molbev/mst010

Kon T., Yoshino T., Mukai T., Nishida M. 2007. DNA sequences identify numerous cryptic species of the vertebrate: a lesson from the gobioid fish *Schindleria*. *Mol. Phylogen. Evol*. 44: 53–62. https://doi.org/10.1016/j.ympev.2006.12.007

Krivenko D. A., Kazanovsky S. G., Vinogradova Yu. K., Verkhozina A. V., Knyazev M. S., Murtazaliev R. A. 2017. In: K. Marhold, J. Kučera (eds.). IAPT/IOPB chromosome data 26. *Taxon* 66(6): 1491–1492. https://doi.org/10.12705/666.30

Krivenko D. A., Kotseruba V. V., Kazanovsky S. G., Verkhozina A. V., Chernova O. D. 2013. In: K. Marhold (ed.). IAPT/IOPB chromosome data 16. *Taxon* 62(6): 1355–1357. https://doi.org/10.12705/626.41

Laumer C. E., Fernández R., Lemer S., Combosch D., Kocot K. M., Riesgo A., Andrade S. C. S., Sterrer W., Sørensen M. V., Giribet G. 2019. Revisiting metazoan phylogeny with genomic sampling of all phyla. *Proc. Biol. Sci*. 286: 20190831. https://doi.org/10.1098/rspb.2019.0831

Lex A., Gehlenborg N., Strobelt H., Vuillemot R., Pfister H. 2014. UpSet: visualization of intersecting sets. *IEEE Trans Vis Comput Graph* 20(12): 1983–1992. https://doi.org/10.1109/TVCG.2014.2346248

Li H. 2013. Aligning sequence reads, clone sequences and assembly contigs with BWA-MEM. *arXiv* 1303.3997v2.

Li H. T., Luo Y., Gan L., Ma P. F., Gao L. M., Yang J. B. et al. 2021. Plastid phylogenomic insights into relationships of all flowering plant families. *BMC Biol*. 19: 232. https://doi.org/10.1186/s12915-021-01166-2

Maia V. H., Gitzendanner M. A., Soltis P. S., Wong G. K., Soltis D. E. 2014. Angiosperm phylogeny based on 18S/26S rDNA sequence data. *Int. J. Pl. Sci*. 175(6): 613–650. https://doi.org/10.1086/676675

Martynenko N., Gusev E., Kapustin D., Kulikovskiy M. 2022. A new cryptic species of the genus *Mychonastes*. *Plants* 11: 3363. https://doi.org/10.3390/plants11233363

Mathew B. 1997. Subgenus *Scorpiris*. In: Species Group of the British Iris Society (ed.). *A guide to species irises*: *their identification and cultivation*. Cambridge: Cambridge University Press. Pp. 225–278.

Maurya S., Sukhramani G., Lee C. Jo S, Kim J., Jeong E. J., Zamora N. A., Garcia R., Zhang Z., Choi S., Choudhary R. K., Kim S. Y. 2025. Comparative plastome evaluation and phylogenomics in Malvaceae. *Sci. Rep*. 15: 24285. https://doi.org/10.1038/s41598-025-07744-6

Mavrodiev E. V., Martínez-Azorín M., Dranishnikov P., Crespo M. B. 2014. At least 23 genera instead of one: the case of *Iris* s. l. *PLOS ONE* 9(8): e106459. https://doi.org/10.1371/journal.pone.0106459

Mayr E. 1942. *Systematics and the Origin of Species*. New York: Columbia Univ. Press. 334 pp.

McLeod D. S. 2010. Of least concern? Systematics of a cryptic species complex: *Limnonectes kuhlii* (Amphibia: Anura: Dicroglossidae). *Mol. Phylogenet. Evol*. 56: 991–1000. https://doi.org/10.1016/j.ympev.2010.04.004

McPherson V. J., Gillings M. R., Ghaly T. M. 2025. Diverse, cryptic, and undescribed: club and coral fungi in a temperate. *Australian forest. J. Fungi*. 11: 502. https://doi.org/10.3390/ jof11070502

Mose L. E., Perou C. M., Parker J. S. 2019. Improved indel detection in DNA and RNA via realignment with ABRA2. *Bioinformatics* 35(17): 2966–2973. https://doi.org/10.1093/bioinformatics/btz033

Murphy N. P., King R. A., Delean S. 2015. Species, ESUs or populations? *Invertebr. Syst*. 29(5): 457–467. https://doi.org/10.1071/IS14036

Müntzing A. 1936. The evolutionary significance of autopolyploidy. *Hereditas*. 21(2–3): 363–378. https://doi.org/10.1111/j.1601-5223.1936.tb03204.x

Nafisi H., Kaveh A., Kazempour-Osaloo S. 2023. Characterizing nrDNA ITS1, 5.8S and ITS2 secondary structures and phylogenetic utility in Hedysareae. *PLOS ONE* 18(4): e0283847. https://doi.org/10.1371/journal.pone.0283847

Onut-Brännström I., Johannesson H., Tibell L. 2018. *Thamnolia tundrae* sp. nov., a cryptic species and putative glacial relict. *The Lichenologist* 50(1): 59–75. https://doi.org/10.1017/S0024282917000615

Padial J. M., Miralles A., De la Riva I. et al. 2010. The integrative future of taxonomy. *Frontiers in Zoology* 7: 16. https://doi.org/10.1186/1742-9994-7-16

Pellicer J., Hidalgo O., Dodsworth S., Leitch I. J. 2018. Genome size diversity and its impact on the evolution of land plants. *Genes* (Basel) 9(2): 88. https://doi.org/10.3390/genes9020088

Pfosser M., Amon A., Lelley T., Heberle-Bors E. 1995. Evaluation of sensitivity of flow cytometry in detecting aneuploidy in wheat using disomic and ditelosomic wheat-rye addition lines. *Cytometry A* 21(4): 387–393. https://doi.org/10.1002/cyto.990210412

Prančl J., Kaplan Z., Trávníček P., Jarolímová V. 2014. Genome size as a key to evolutionary complex aquatic plants: polyploidy and hybridization in *Callitriche* (Plantaginaceae). *PLOS ONE* 9(9): e105997. https://doi.org/10.1371/journal.pone.0105997

Probatova N. S. 2006. Chromosome numbers of plants of the Primorye Territory, the Amur River basin and Magadan Region. *Bot. Zhurn*. 91(3): 491–509. [In Russian] (***Пробатова Н. С.*** Числа хромосом растений Приморского края, бассейна Амура и Магаданской области // Бот. журн., 2006. Т. 91, № 3. С. 491–509).

Probatova N. S., Barkalov V. Yu., Rudyka E. G., Tzyrenova D. Yu., Seledets V. P. 2012a. In: K. Marhold (ed.). IAPT/IOPB chromosome data 14. *Taxon* 61(6): 1341–1342. https://doi.org/10.1002/tax.616027

Probatova N. S., Kazanovsky S. G., Barkalov V. Yu., Rudyka E. G., Shatokhina A. V. 2015. In: K. Marhold (ed.). IAPT/IOPB chromosome data 20. *Taxon* 64(6): E30–E32. https://doi.org/10.12705/646.42

Probatova N. S., Kazanovsky S. G., Rudyka E. G., Seledets V. P., Nechaev V. A. 2012b. In: K. Marhold (ed.). IAPT/IOPB chromosome data 14. *Taxon* 61(6): 1342–1344. https://doi.org/10.1002/tax.616027

Probatova N. S., Rudyka E. G., Seledets V. P., Nechaev V. A. 2008. In: K. Marhold (ed.). IAPT/IOPB chromosome data 6. *Taxon* 57(4): 1268–1271. https://doi.org/10.1002/tax.574017

Punina E. O., Nosov N. N., Myakoshina Y. A., Rodionov A. V., Gnutikov A. A., Shmakov A. I., Olonova M. V.

2016. New octoploid *Catabrosa* (Poaceae) species from Altai. *Kew Bull*. 71(3): 35. https://doi.org/10.1007/s12225-016-9646-5

Renner S. S. 2016. The use of DNA characters in the formal naming of species. *Syst. Biol.* 65(6): 1086–1095. https://doi.org/10.1093/sysbio/syw032

Rideout J. R., Bolyen E., McDonald D., Baeza Y., V, Alastuey J. C., Pitman A. et al. 2025. Scikit-bio 0.7.1.post1. *Zenodo*. https://doi.org/10.5281/zenodo.17487690

Robinson J., Thorvaldsdóttir H., Winckler W., Guttman M., Lander E. S., Getz G., Mesirov J. P. 2011. Integrative genomics viewer. *Nat. Biotechnol*. 29: 24–26. https://doi.org/10.1038/nbt.1754

Rodionov A. V., Amosova A., Belyakov E., Zhurbenko P., Mikhaylova Y., Punina E., Shneyer V., Loskutov I., Muravenko O. 2019. Genetic consequences of interspecific hybridization, its role in speciation and phenotypic diversity of plants. *Russ. J. Genet*. 55(3): 278–294. https://doi.org/10.1134/S1022795419030141

Ronquist F., Teslenko M., Mark P., Ayres D., Darling A., Höhna S., Larget B., Liu L., Suchard M., Huelsenbeck J. 2012. MrBayes 3.2: Efficient Bayesian phylogenetic inference and model choice across a large model space. *Systematic Biology* 61: 539–542. https://doi.org/10.1093/sysbio/sys029

Schüßler D., Blanco M. B., Guthrie N. K., Sgarlata G. M., Dammhahn M., Ernest R. et al. 2024. Morphological variability or inter-observer bias? *Am. J. Biol. Anthrop*. 183(1): 60–78. https://doi.org/10.1002/ajpa.24836

Shatokhina T. A. 2006. Chromosome numbers of some plants of the Amur Region flora. *Bot. Zhurn*. 91(3): 487–490. [In Russian] (***Шатохина Т. А.*** Числа хромосом некоторых растений флоры Амурской области // Бот. журн., 2006. Т. 91, № 3. С. 487–490).

Shen J., Zhang X., Landis J. B., Zhang H., Deng T., Sun H., Wang H. 2020. Plastome evolution in *Dolomiaea* using phylogenomic and comparative analyses. *Front. Plant Sci*. 11: 376. https://doi.org/10.3389/fpls.2020.00376

Shen Y., Wang Z., Guan K. 2007. Karyotypical studies on thirteen *Iris* plants from China. *J. Syst. Evol*. 45(5): 601–618. https://doi.org/10.1360/aps06064

Shneyer V. S., Kotseruba V. V. 2015. Cryptic species in plants and their detection by genetic differentiation between populations. *Russ. J. Genet.* 5(5): 528–541. https://doi.org/10.1134/S2079059715050111

Shneyer V. S., Punina E. O., Rodionov A. V. 2018. Intraspecific variation of ploidy in angiosperms and its taxonomical treatment. *Bot. Zhurn*. 103(5): 555–585. [In Russian] (***Шнеер В. С., Пунина Е. О., Родионов А. В.*** Внутривидовые различия в плоидности у покрытосеменных и их таксономическая интерпретация // Бот. журн., 2018. Т. 103, № 5. С. 555–585.

Simpson G. G. 1951. The species concept. *Evolution* 5: 285–298.

Skaptsov M. V., Kutsev M. G., Smirnov S. V., Vaganov A. V., Uvarova O. V., Shmakov A. I. 2024. Standards in plant flow cytometry: an overview, polymorphism and linearity issues. *Turczaninowia* 27, 2: 86–104. https://doi.org/10.14258/turczaninowia.27.2.10

Sokoloff D. D., Marques I., Macfarlane T. D., Remizowa M. V., Lam V. K. Y., Pellicer J., Hidalgo O., Rudall P. J., Graham S. W. 2019. Cryptic species in an ancient flowering-plant lineage (Hydatellaceae, Nymphaeales) revealed by molecular and micromorphological data. *Taxon* 68(1): 1–19. https://doi.org/10.1002/tax.12026

Soltis P. S., Soltis D. E., Wolf P. G., Nickrent D. L., Chaw S. M., Chapman R. L. 1999. The phylogeny of land plants inferred from 18S rDNA sequences. *Mol. Biol. Evol*. 16(12): 1774–1784. https://doi.org/10.1093/oxfordjournals.molbev.a026089

Stamatakis A. 2014. RAxML version 8: A tool for phylogenetic analysis and post-analysis of large phylogenies. *Bioinformatics* 30: 1312–1313.

Stayton C. T. 2006. Testing hypotheses of convergence with multivariate data. *Evolution* 60(4): 824–841.

Stepanov N. V., Muratova E. N. 1995. Chromosome numbers of some vascular plant taxa from the Krasnoyarsk Territory. *Bot. Zhurn*. 80(6): 114–116. [In Russian] (***Степанов Н. В., Муратова Е. Н.*** Хромосомные числа некоторых таксонов высших растений Красноярского края // Бот. журн., 1995. Т. 80, № 6. С. 114–116).

Strand M., Sundberg P. 2011. A DNA-based description of a new Nemertean species. *Marine Biology Research* 7(1): 63–70. https://doi.org/10.1080/17451001003713563

Struck T. H., Feder J. L., Bendiksby M., Birkeland S., Cerca J., Gusarov V. I. et al. 2018. Finding evolutionary processes hidden in cryptic species. *Trends Ecol. Evol.* 33(3): 153–163. https://doi.org/10.1016/j.tree.2017.11.007

Swift H. F., Gómez Daglio L., Dawson M. N. 2016. Three routes to crypsis: stasis, convergence, and parallelism in the *Mastigias* species complex. *Mol. Phyl. Evol*. 99: 103–115. https://doi.org/10.1016/j.ympev.2016.02.013

Tayier G., Hasimu D., Aishan T., Yimingniyazi A. 2024. Impact of a heterogeneous environment on the population expansion of *Iris ruthenica* in high mountain grasslands. *Front. Plant Sc*. 15: 1363496. https://doi.org/10.3389/fpls.2024.1363496

Techaprasan J., Klinbunga S., Kanlayanapaphon C., Jenjittikul T. 2010. Genetic variation of *Kaempferia* in Thailand based on chloroplast DNA sequences (*psbA-trnH*, *petA-psbJ*). *Genet. Mol. Res*: *GMR* 9: 1957–1973. https://doi.org/10.4238/vol9-4gmr873

Tillie N., Chase M. W., Hall T. 2000. Molecular studies in the genus *Iris* L.: a preliminary study. *Ann. Bot*. (*Roma*) 58: 105–112. https://doi.org/10.4462/annbotrm-9068

Van der Auwera G. A., O'Connor B. D. 2020. *Genomics in the Cloud*: *Using Docker*, *GATK*, *and WDL in Terra*. Sebastopol, CA: O'Reilly Media. 467 pp.

Wang Y., Zhou Q. S., Qiao H. J., Zhang A. B., Yu F., Wang X. B., Zhu C. D., Zhang Y. Z. 2016. Formal nomenclature and description of cryptic species of the *Encyrtus sasakii* complex. *Sci. Rep*. 6: 34372. https://doi.org/10.1038/srep34372

Wheeler A. S., Wilson C. A. 2014. Exploring phylogenetic relationships in a Northern Hemisphere group of semi-aquatic *Iris*. *Syst. Bot*. 39(3): 759–766. https://doi.org/10.1600/036364414X681482

Wiens J. J., Ackerly D. D., Allen A. P., Anacker B. L., Buckley L. B., Cornell H. V. et al. 2010. Niche conservatism as an emerging principle in ecology and conservation biology. *Ecol. Lett*. 13(10): 1310–1324. https://doi.org/10.1111/j.1461-0248.2010.01515.x

Wiley E. O. 1981. Remarks on Willis' species concept. *Syst. Zool*. 30: 86–87.

Wilson C. A. 2004. Phylogeny of *Iris* based on chloroplast *matK* and *trnK* intron. *Mol. Phyl. Evol.* 33: 402–412. https://doi.org/10.1016/j.ympev.2004.06.013

Wilson C. A. 2011. Subgeneric classification in *Iris* re-examined using chloroplast sequence data. *Taxon* 60: 27–35. https://doi.org/10.1002/tax.601004

Wilson C. A., Guo J. 2013. Molecular phylogenetic study of the crested *Iris* based on five plastid markers. *Syst. Bot*. 38: 987–995.

Wilson C. A., Padiernos J., Sapir Y. 2016. The royal irises: plastid and low-copy nuclear data. *Taxon* 65: 35–46. https://doi.org/10.12705/651.3

Zhao Y., Noltie H. J., Mathew B. 2002. Iridaceae A. L. Jussieu. In: *Flora of China* (eFloras). St. Louis: Missouri Botanical Garden, Cambridge: Harvard University Herbaria. URL: http://www.efloras.org (Accessed November 2025).

Zheng Y., Meng T., Bi X., Lei J. 2017. Investigation and evaluation of wild *Iris* resources in Liaoning Province, China. *Genet. Res. Crop Evol*. 64: 967–978. https://doi.org/10.1007/s10722-016-0418-8

Zhurbenko P. M., Badaeva E. D., Alexeeva N. B., Kotseruba V. V. 2023. In: K. Marhold, J. Kučera (eds.). IAPT chromosome data 41. *Taxon* 72(6): 1396. https://doi.org/10.1002/tax.13104

Ziegler A., Li X., Wiens J. 2025. The evidence for new species across the Tree of Life: Morphology still rules the largest kingdoms. *BSSB* 4(1). https://doi.org/10.18061/bssb.v4i1.10466

Zuntini A. R., Carruthers T., Maurin O., Bailey P. C., Leempoel K., Brewer G. E., et al. 2024. Phylogenomics and the rise of the angiosperms. *Nature* 629: 843–850. https://doi.org/10.1038/s41586-024-07324-0